2187

Spectroscopy, Thermal and Optical Properties of Nd^{3+} Doped Chalcogenide Glasses

S.M. Lima[a*], J.A. Sampaio[a], T. Catunda[a], A.S.S. de Camargo[a], L.A.O. Nunes[a], M.L. Baesso[b] and D.W. Hewak[c]

[a] *Instituto de Física de São Carlos, Universidade de São Paulo - USP, CEP 13560-970, São Carlos-SP, Brazil*

[b] *Departamento de Física, Universidade Estadual de Maringá - UEM, CEP 87020-900, Maringá-PR, Brazil*

[c] *Optoelectronics Research Centre, University of Southampton, Southampton SO17 1BJ, England, UK*

Abstract

We investigated the spectroscopic, thermo-optical and mechanical properties of 70%Ga_2S_3:30%La_2S_3 (mole %) chalcogenide glass and glasses doped with 0.05, and 0.2 mole % Nd_2S_3, prepared by melt-quenching the sulphides in a vitreous carbon crucible in a silica ampoule. The fluorescence quantum efficiency for the 0.05 mole % Nd^{3+} doped sample, obtained by thermal lens technique was (1.01 ± 0.08) and the lifetime of this sample was (78.00 ± 0.05)μs. The thermal diffusivity of these samples (2.7 ± 0.1)×10^{-3} cm^2s^{-1} were determined by the thermal lens method.

*Corresponding author. Fax: +55-16 271 3616; e-mail: smlima@if.sc.usp.br

1. Introduction

Chalcogenide glasses are interesting materials due to their fusion temperature, optical transparence window, linear and non linear refractive indices, phonon energy ~425 cm^{-1}, and non-radiative decay rates of rare-earth energy levels [1,2]. These properties make them interesting for optical amplifiers and photonic devices. We mention that laser action in Nd^{3+} doped chalcogenide glasses has been observed in rectangular samples [3] and fiber [4]. In both cases, laser performance was affected by thermal lens (TL) effects. The determination of fluorescence quantum efficiency, η, especially for solid samples, has been shown to be difficult and results in the literature are controversial [5] mainly due to the limitations of the employed experimental methods. Some of the methods employed to measure this parameter include photothermal techniques such as photoacoustic spectroscopy and calorimetry [6]. In a recent work Baesso et al. [7] used the TL technique to determine η for low silica content calcium aluminosilicate glasses doped with different concentrations of neodymium.

Previously, the TL technique had also proved to be a convenient method to determine thermal diffusivity, D, and temperature coefficient of optical path length, ds/dT, for transparent materials [7-10]. The TL effect is caused by deposition of heat through a non radiative decay process after the laser energy has been absorbed by the sample. This heat produces a temperature gradient perpendicular to the beam direction, which affects the wave front of a TEM_{00} probe laser beam, whose energy in the perpendicular direction is fitted by a Gaussian function. By measuring this variation on the far field, the thermal optical properties can be determined [7-10].

The aim of this work, was to determine the thermal properties such as D, ds/dT and η, of 70 mole %Ga_2S_3:30 mole %La_2S_3 samples with 0, 0.05 and 0.2 mole % of Nd_2S_3

using the TL technique. In addition, we also measured optical absorption and emission spectra, and lifetime of $^4F_{3/2}$ level, to obtain the fluorescence quantum efficiency via Judd Ofelt (JO) calculations. Furthermore, measurements of physical properties such as Vickers microhardness, H_v, density, ρ, specific heat, α, glass transition temperature, T_g, and glass crystallization temperature, T_x, measurements are also presented.

2. Theory

2.1. Judd Ofelt theory

The radiative properties of rare-earth ions in a variety of different host materials can be described by the JO theory [11,12]. This theory is well established in the literature, so we will only be concerned with the topics necessary to analyze our results. By assuming the experimental (F_{exp}) and theoretical (F_{calc}) oscillator strengths [13] are equal,

$$\frac{mc}{\pi e^2 N}\int \alpha(\nu)d\nu = \frac{8\pi^2 m(n^2+2)^2}{27nh}\frac{\nu}{(2J+1)}\sum_{\lambda=2,4,6}\Omega_\lambda \left|\langle aJ|U^\lambda|bJ'\rangle\right|^2 \qquad (1)$$

where m is the electron mass, c is the speed of light, e is the electron charge, N is the number of ions per cm^3, $\int \alpha(\nu)d\nu$ is the area of the absorption band, n is the refractive index, h is the Planck's constant, ν is the transition frequency, J is the ground state quantum number, Ω_λ are the intensity parameters, $\langle aJ|U^\lambda|bJ'\rangle$ are the reduced matrix elements of the tensor operator, U^λ, of rank, λ. We can obtain, for this case, Ω_2, Ω_4 and Ω_6. Since Nd^{3+} the transitions are assumed to be pure electric dipole [13], only this term of the potential was considered in Eq. (1).

In spite of the controversy about the physical meaning of Ω_λ parameters, the

variations in the Ω_2, Ω_4 and Ω_6 values can be attributed to changes in the chemical environment around a rare earth ion [14]. These intensity parameters can be applied to calculate the line strengths corresponding to the transitions from $^4F_{3/2} \rightarrow {}^4I_{9/2}$, $^4I_{11/2}$, $^4I_{13/2}$ and $^4I_{15/2}$ of the Nd^{3+} ion. Using the line strengths, the radiative transition rates between two given levels, a and b, $A(aJ \rightarrow bJ')$, can be calculated as [13],

$$A(aJ,bJ') = \frac{64\pi^4\nu^3}{3(2J+1)hc^3}\frac{n(n^2+2)^2}{9}e^2\sum_{\lambda=2,4,6}\Omega_\lambda\left|\langle aJ|U^\lambda|bJ'\rangle\right|^2 \quad (2)$$

and from $A(aJ,bJ')$ probabilities we can calculate the luminescence branching ratios, $\beta(aJ,bJ')$, as well as the radiative lifetime (τ_0) as [13],

$$\beta(aJ;bJ') = \frac{A(aJ,bJ')}{\sum_{J'}A(aJ;bJ')} \quad (3)$$

and

$$\tau_0 = \frac{1}{\sum_{S,L,J}A(aJ;bJ')}. \quad (4)$$

The fluorescence quantum efficiency of the transitions can be determined from the ratio between the measured lifetime (τ) and the radiative lifetime (τ_0): $\eta_{JO} = \tau/\tau_0$.

2.2. Thermal Lens Theory

In the two beams mode mismatched TL technique, the sample is illuminated by two TEM_{00} Gaussian laser beams as shown in Fig. 1. The excitation laser beam (Ti:sapphire laser) produces a local temperature increase within the sample creating a lenslike element in the heated region. When the probe beam (HeNe laser) passes thorough the created lens, its

optical path length undergoes a temporal change that can be observed measuring the beam center intensity in the far field. Using Fresnel diffraction theory [15], an analytical expression can be obtained for the probe beam intensity change, $I(t)$ [9],

$$I(t) = I(0)\left\{1 - \frac{\theta}{2}\tan^{-1}\left[\frac{2mV}{\left[(1+2m)^2 + V^2\right]t_c/2t + 1 + 2m + V^2}\right]\right\}^2 \tag{5}$$

where

$$m = \left(\frac{w_p}{w_e}\right)^2 \quad ; \quad V = \frac{Z_1}{Z_{cp}} \quad when \quad Z_{cp} << Z_2 . \tag{6}$$

Here, w_p and w_e are the probe beam radius and excitation laser beam radius at the sample, respectively, Z_1 is the distance between the probe beam focal plane and the sample, Z_{cp} is the confocal distance of the probe beam, Z_2 is the distance between the sample and the detector and $I(0)$ is the $I(t)$ when the transient time t or θ is zero. In the steady state, the on-axis probe beam intensity change is proportional to the phase shift, θ, induced by TL, which is approximately given by [9],

$$\theta = -\frac{PAL_{eff}}{K\lambda_p}\varphi\frac{ds}{dT} \tag{7}$$

where P is the excitation laser power, K is the thermal conductivity, λ_p is the probe beam wavelength, L is the sample thickness, effective length is $L_{eff} = (1-e^{-AL})/A$, ds/dT is the temperature coefficient of the optical path length change, A is the absorption coefficient and φ is the fraction of absorbed energy converted into heat per photon. For the undoped sample all absorbed energy is converted into heat, so $\varphi = 1$. For fluorescent samples, like the Nd^{3+} doped glasses studied in this work, $\varphi = 1 - \eta\lambda_{exc}/\langle\lambda_{em}\rangle$, where η is the sample

radiative quantum efficiency, λ_{exc} is the excitation beam wavelength, and $<\lambda_{em}>$ is the average wavelength of the fluorescence.

The characteristic TL signal response time, t_c, is given by [9] as,

$$t_c = \frac{w_e^2}{4D} \tag{8}$$

where $D = K/\rho\alpha$ is the thermal diffusivity, K is the thermal conductivity, ρ is the density and α is the specific heat.

3. Experimental

Samples were prepared in the molar composition 70%Ga_2S_3 and 30%La_2S_3 (GLS) by melt-quenching the sulphides in a vitreous carbon crucible in a silica ampoule. The Nd_2S_3 dopant concentration in the doped samples are 0.05 and 0.2 mole%. The samples were cut in disks of 10 mm diameter and 1.5 mm thickness and optically polished.

Density was measured at room temperature using the buoyancy method based on the Archimede's principle with CCl_4 as the immersion liquid, whereas Vickers hardness was measured using a microhardness tester (Leitz Wetzlar). To minimize the experimental errors, at least 15 indentations were made, using loads of 30 g. The specific heat measurements were performed using the relaxation method in a conventional calorimeter [16,17]. The determination of T_g and T_x was carried out using 100 mg samples in a simultaneous thermal analyzer (Netzsch, STA 409- EP).

Absorption spectra were obtained at room temperature, using a spectrophotometer (Perkin Elmer Lambda 900) over the range of 500 to 1200 nm. Spectra were normalized to obtain the absorption coefficient. Fluorescence spectra were obtained at room temperature

using a diode laser as excitation source at around 808 nm, and the luminescence signal was detected by an InGaAs detector operating at 77 K, in the range of 800 to 1500 nm. Lifetime measurements of level $^4F_{3/2}$ were performed using a rhodamine dye laser, pumped by a 5 ns pulsed nitrogen laser, being the luminescence signal intensity measured with a digital oscilloscope.

Fig. 1 shows a mode-mismatched thermal lens experimental setup. This experiment was made using a Ti:sapphire laser at 814 nm to produce the TL effect at the sample. The laser beam was focused by a lens (L_1) with focal length f = 20 cm and the sample was placed at its focal plane. Exposure of the sample to excitation beam was controlled by means of a chopper with frequency around 5Hz. The probe laser beam was a HeNe laser at λ_p = 632.8 nm. It was also focused by a lens (L_2) with focal length f = 20 cm at an angle $\gamma <$ 1.5° with respect to the excitation beam. The excitation and probe beams radii at the sample were measured with a meter (Thorlabs omega model WM100), giving $w_e = (4.95 \pm 0.09) \times 10^{-3}$ cm and $w_p = (18.2 \pm 0.3) \times 10^{-3}$ cm, respectively. Using these quantities in Eq. (6), m = (13.5 ± 0.6) was obtained. The probe beam minimum radius, w_0, was measured with the same meter and from its magnitude, $Z_{cp} = \pi w_0^2/\lambda_p$, where λ_p is the probe wavelength, could be calculated as (4.09 ± 0.08) cm. Choosing the distance between the sample and the probe beam waist, Z_1, as (7.10 ± 0.05) cm and using $V = Z_1/Z_{cp}$ (Eq. (6)), V = (1.73 ± 0.04) was obtained. The excitation beam, after passing through the sample, was incident on a photodiode (D_1) and used as trigger in the acquisition program. These adjustable mirrors, M_3, M_4 and M_5 were used to get an approximate 2 m optical path length from the sample to an iris mounted before the photodiode (D_2). This iris was put in front of the detector to select the central part of the probe beam. The experimental error introduced by the equipments resolutions for all the spectroscopic measurements is 5% at the maximum.

4. Results

4.1. Physical Properties

Fig. 2 shows the thermal relaxation curve obtained for the set, sample (undoped GLS glass) and silicon holder (heat capacity C_h = 43.151 mJK^{-1}) [17]. The dissipated power was, P_d = 616 μW. This data was fitted by the equation $\Delta T = \Delta T_{max}\, e^{-t/\tau}$ [17] giving ΔT_{max} = (0.119 ± 0.001) K and τ = (9.92 ± 0.05) s. The correlation coefficient of the fit was R = 0.9967. Since the heat capacity is given by $C = \frac{P_d.\tau}{\Delta T}$ [17], C_{s+h} = (51.3 ± 0.7) mJK^{-1} was obtained for the set sample (s) and holder (h). With these and the mass of the sample 15.16 mg, the specific heat α = (0.54 ± 0.04) $Jg^{-1}K^{-1}$ could be calculated from $\alpha = \frac{C_{s+h} - C_h}{m}$ [17]. This procedure was carried out five times for each sample, the deviation error was ± 5%. These quantities are in agreement to within errors of measurement with the literature [18]. Table 1 presents the results for density, ρ, Vickers microhardness, H_v, specific heat, α, T_g and T_x for the GLS glass. Only changes < 10% in these physical parameters were observed.

4.2. Spectroscopic Results

The ground state absorption spectrum for a 0.2 mole% Nd^{3+} doped GLS glass is shown in Fig. 3. We note, the UV absorption edge of this glass is around 500 nm and 6 transitions are resolved. Emission spectra were obtained by pumping the samples at 815 nm ($^2H_{9/2}$ and $^4F_{5/2}$ levels) to populate level $^4F_{3/2}$ from which the laser transition at 1080 nm originates [19]. These levels were chosen for excitation since their absorption coefficients are about three times larger than that of $^4F_{3/2}$ level.

From the absorption spectrum, the JO intensity parameters were calculated giving: $\Omega_2 = (9.2 \pm 0.2)\times10^{-20}$; $\Omega_4 = (7.3 \pm 0.3)\times10^{-20}$; and $\Omega_6 = (4.9 \pm 0.1)\times10^{-20}$ cm^2, and the root means square error (rms_{error}) is 2.0%. The transition probabilities from $^4F_{3/2}$ to the lower lying levels and the calculated branching ratios are presented in Table 2.

Fig. 4 presents the emission spectrum of the 0.2 mole% Nd^{3+} doped sample, in which the bands corresponding to transitions from $^4F_{3/2}$ to the lower lying $^4I_{9/2}$, $^4I_{11/2}$ and $^4I_{13/2}$ levels, as shown in the inset, can be observed. The $^4F_{3/2} \rightarrow {}^4I_{15/2}$ transition was not observed.

For the 0.05 and 0.2 mole% Nd^{3+} doped samples, the measured lifetimes are (78.00 ± 0.05) μs and (75.00 ± 0.04) μs respectively. By JO calculations, the radiative lifetime, τ_0, obtained was (78 ± 7) μs. With these lifetimes quantum efficiencies for the doped samples could be determined and are shown in Table 3.

4.3. Thermo-optical properties

Fig. 5 shows typical TL data for the undoped GLS sample. The dots are the experimental data and the correlation coefficient of the fit by Eq. (5) is R > 0.9999, giving θ = -(0.1009 ± 0.0002) rad and t_c = (2.30 ± 0.02) ms with. Using Eq. (8) for t_c with w_e = = (4.95 ± 0.09)×10^{-3} cm, it was possible to obtain $D = (2.7 \pm 0.1)\times10^{-3}$ cm^{2}s^{-1}. With the D and the measured ρ and α in Table 1, the thermal conductivity for this sample was calculated as $K = (5.9 \pm 0.3)\times10^{-3}$ WK^{-1}cm^{-1}. The same procedure was developed for the other samples and these parameters are independent of concentration in this range. Using Eq. (7), the above cited θ, determined by the transient and the calculated K jointly with P = 6 mW, A = (0.63 ± 0.01) cm^{-1}, L = (0.138 ± 0.001) cm, AL_{eff} = 0.0833 and $\lambda_p = 632.8\times10^{-7}$ cm, the temperature coefficient of the optical path length change is, $ds/dT = (7.5 \pm 0.6)\times10^{-5}$ K^{-1}.

To determine the fluorescence quantum efficiency, it is necessary to know the fluorescence average wavelength $<\lambda_{em}>$. It can be calculated by $\langle\lambda_{em}\rangle = \sum_i \beta_i \lambda_i$ where β_i is the branching ratio of $^4F_{3/2} \rightarrow {}^4I_J$ (J = 15/2, 13/2, 11/2 and 9/2) transitions, and λ_i is the wavelength of each transition. Using the branching ratios determined by JO (Table 2), $<\lambda_{em}>$ = 1011.7 nm was found. Since *ds/dT* is independent of doping at our concentrations, *ds/dT* could be used to determine φ for the samples doped with 0.05 and 0.2 mole% of Nd^{3+}, giving φ = (0.19 ± 0.01) and (0.17 ± 0.01), respectively. Since $\varphi = 1 - \eta\lambda_{exc}/\langle\lambda_{em}\rangle$, the fluorescence quantum efficiencies determined for these samples were η = (1.01 ± 0.08) and (1.03 ± 0.09) as shown in Table 3.

5. Discussion

It is interesting to us to notice that the covalence, typical of chalcogenide glasses, associated with a refractive index ~2.4 increased intensity of the absorption band at 600 nm ($^2G_{7/2}$, $^4G_{5/2}$ levels), as shown in Fig. 3. That is due to an increase in the intensity of the hypersensitive transition $^4I_{9/2} \rightarrow {}^4G_{5/2}$ [20]. The emission band corresponding to $^4F_{3/2} \rightarrow {}^4I_{15/2}$ transition could not be observed because of the cross relaxation ($^4F_{3/2}$, $^4I_{9/2} \rightarrow {}^4I_{15/2}$, $^4I_{15/2}$) as shown in the inset of Fig. 4 [20, 21]. This cross relaxation is even larger when the Nd^{3+} concentration increases, providing a decrease in lifetime. Besides, at the larger excitation powers there is a larger probability of interaction between two excited ions providing an additional decay channel for the $^4F_{3/2}$ level, via visible upconverted emission from the $^2G_{9/2}$, $^4G_{7/2}$ levels [22].

The thermal diffusivity for these samples is similar to ZBLAN glass [8], but the thermal conductivity is ~ 1.6 times less. That is due to the smaller density and specific heat

of GLS glass since $K=\rho\alpha D$. Our results for D are in agreement with previous work [10] to within ± 3%. The *ds/dT* for chalcogenide glass was positive, whereas for fluoride glasses it is negative [8, 10]. Even so, the absolute *ds/dT* for chalcogenide glass is one order of magnitude larger than the *ds/dT* obtained for fluorides. This difference makes the optical path of chalcogenide glass more susceptible to temperature changes. The smaller thermal conductivity and larger *ds/dT* of these chalcogenide glasses compared to those of fluoride glasses are responsible for the larger thermal lens effects observed [3,4,13]

The results of quantum efficiency obtained by JO and by TL method are in good agreement. It is worth noting that experimental branching ratios were also obtained from the emission spectrum and their ratios are presented in Table 2. If these ratios are used to determine the average emission wavelength, the quantum efficiency increases by a factor of 4%, which is within our experimental error (10%). The difference between experimental and JO calculated branching ratios can be explained by a decrease in the transition probability of $^4F_{3/2} \rightarrow {}^4I_{9/2}$ transition, probably due to a process of reabsorption from ground state $^4I_{9/2}$. Judd Ofelt theory does not take account of such a process, therefore a larger branching ratio is obtained.

6. Conclusions

The TL technique has been used to measure η for Nd^{3+} doped solid samples, that is, GLS chalcogenide glasses. Besides, *D*, *K* and *ds/dT* parameters were also determined. The samples had a thermal diffusivity similar to the ZBLAN glass [8] and their fluorescence quantum efficiencies obtained by JO and TL are in good agreement. The absolute *ds/dT* for chalcogenide glass is positive and one order of magnitude larger than that obtained for fluorides [8], making the former more susceptible to temperature changes.

Acknowledgements

Authors are thankful to FAPESP, CNPq, and CAPES agencies, for the financial support of this work.

References

[1] P.N. Kumta and S.H. Risbud, J. Mat. Science 29 (1994) 1135.

[2] G. Fuxi, J. Non-Cryst. Solids 140 (1992) 184.

[3] D.W. Hewak, R.C. Moore, T. Schweizer, J. Wang, B. Samson, W.S. Brocklesby, D.N. Payne and E.J. Tarbox, Elect. Lett. 32 (1996) 384-385.

[4] T. Schweizer, B.N. Samson, R.C. Moore, D.W. Hewak and D.N. Payne, Elect. Lett. 33(5) (1997) 414.

[5] A. Mandelis, J. Vanniasinkan and S. Budhudu, Phys. Rev. B. 48 (1993) 6808.

[6] R.S. Quimby and W.M. Yen, Opt. Lett. 3 (1978) 181.

[7] M.L. Baesso, A.C. Bento, A.A. Andrade, J.A. Sampaio, E. Pecoraro, L.A.O. Nunes, T. Catunda and S. Gama, Phys. Rev. B 57(17) (1998) 10545.

[8] S.M. Lima, T. Catunda, R. Lebullenger, A.C. Hernandes, M.L. Baesso, A.C. Bento and L.C.M. Miranda, Phys. Rev. B 60 (1999) 15173.

[9] M.L. Baesso, J. Shen and R.D. Snook, J. Appl. Phys. 75 (1994) 3732.

[10] S.M. Lima, T. Catunda, M.L. Baesso, L.D. Villa, Y. Messadeq, E.B. Stucchi and S.J.L. Ribeiro, J. Non-Cryst. Solids 247 (1999) 222.

[11] M.B. Saisudha and J. Ramakrishna, Phys. Rev. B 53 (1996) 6186.

[12] A.A. Kaminskii, G. Boulon, M. Buoncristisni, B. Di Bartolo, A. Kornienko and V.Mironov, Phys. Stat. Sol. (A) 141 (1994) 471.

[13] B. Viana, M. Palazzi and O. LeFol, J. Non-Cryst. Solids 215 (1997) 96.

[14] C.K. Jorgensen and R. Reisfeld, J. Less-Common Met. 93 (1983) 107.

[15] S.J. Sheldon, L.V. Knight and J.M. Thorne, Appl. Opt. 21 (1982) 1663.

[16] R. Bachmann, F. J. Disalvo Jr., T. H. Geballe, R. L. Greene, R. E. Howard, C. N. King, H. C. Kirsch, K. N. Lee, R. E. Scwall, H. U. Thomas and R. B. Zubeck, The Review of Scientific Instruments 43 (1972) 205.

[17] L. S. Azechi, R. F. da Costa, A. N. Medina and F. C. G. Gandra, Revista de Física Aplicada e Instrumentação 10 (1995) 70.

[18] P. Klocek, Handbook of Optical materials, Marcel Dekker Inc, New York (1991) 185.

[19] J.S. Sanghera, I.D. Aggarwal, J. Non-Cryst. Solids 256&257 (1999) 6.

[20] T. Schweizer, in: Dan Hewak, (Ed.) Nato. On Properties, Processing and Applications of Glasses and Rare-Earth Doped Glasses for Optical Fibers, Part D - Chalcogenide Glass, p. 320. An INSPEC publication, 1998.

[21] H.G. Danielmeyer, M. Blatte, and P. Balmer, Appl. Phys. 1 (1973) 269.

[22] S.R. Bullock, B.R. Reddy, C.L. Pope, S.K. Nash-Stevenson, J. Non-Cryst. Solids 212 (1997) 85.

Figure Captions

Fig. 1: Schematic diagram of the mode-mismatched thermal lens experimental apparatus, where M_1, M_2, M_3, M_4 and M_5 are mirrors, D_1 and D_2 are photodiodes, and L_1 and L_2 are lenses.

Fig. 2: Thermal relaxation curve obtained for the set, sample (undoped GLS glass) and silicon holder. The line indicates the linear fit, where the correlation coefficient is R = 0.9967.

Fig. 3: Absorption spectrum of 0.2 mol% Nd^{3+} doped GLS obtained at 300 K.

Fig. 4: Emission spectrum of 0.2 mol% Nd^{3+} doped GLS obtained at 300 K. The inset shows a partial energy level diagram indicating transitions from $^4F_{3/2}$ level and the cross relaxation ($^4F_{3/2}$, $^4I_{9/2} \rightarrow {}^4I_{15/2}$, $^4I_{15/2}$) process.

Fig. 5: Transient thermal lens signal for the undoped chalcogenide glass. The line indicates the curve fitting using Eq. (5).

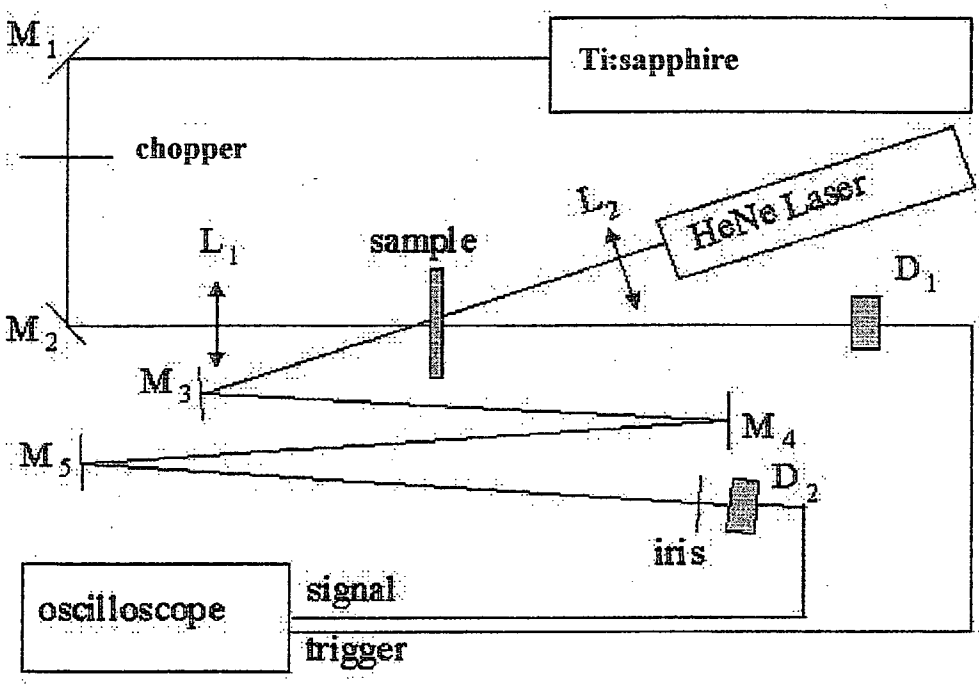

Figure 1: Lima et al.

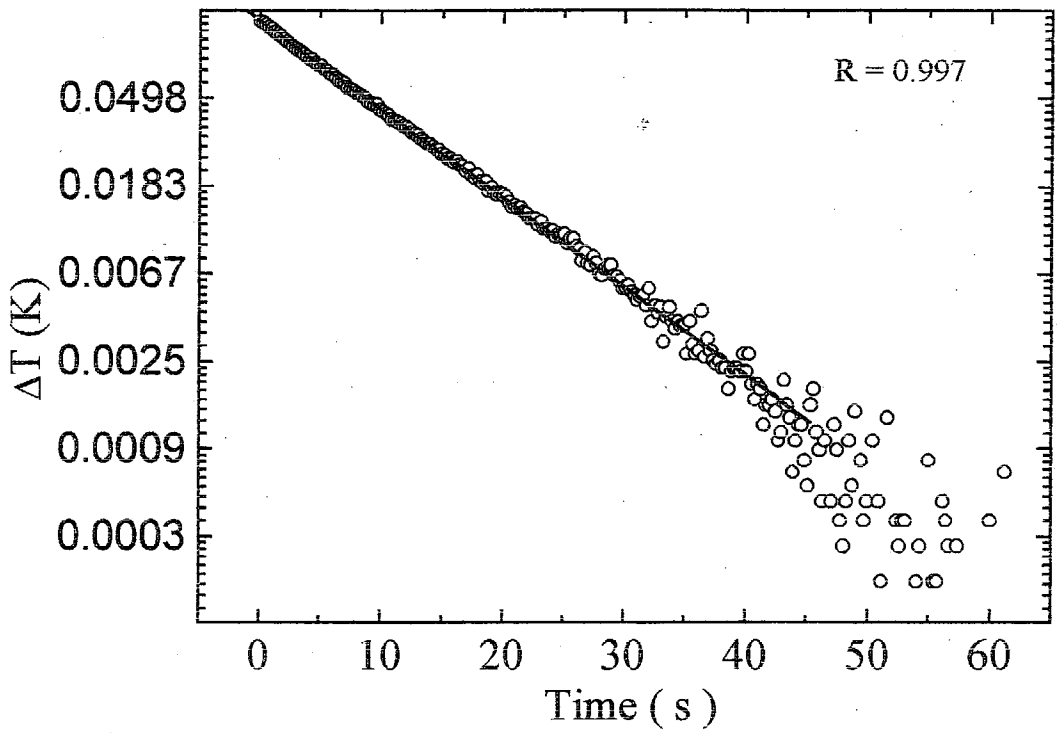

Figure 2: Lima et al.

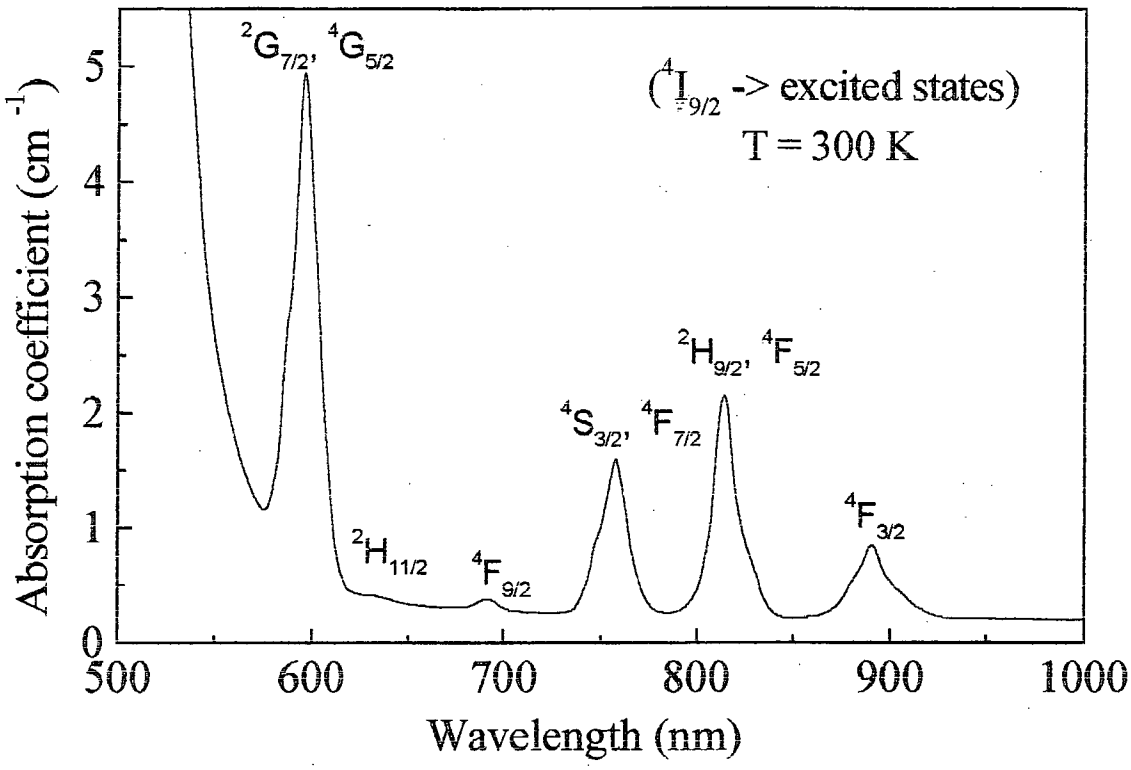

Figure 3: Lima et al.

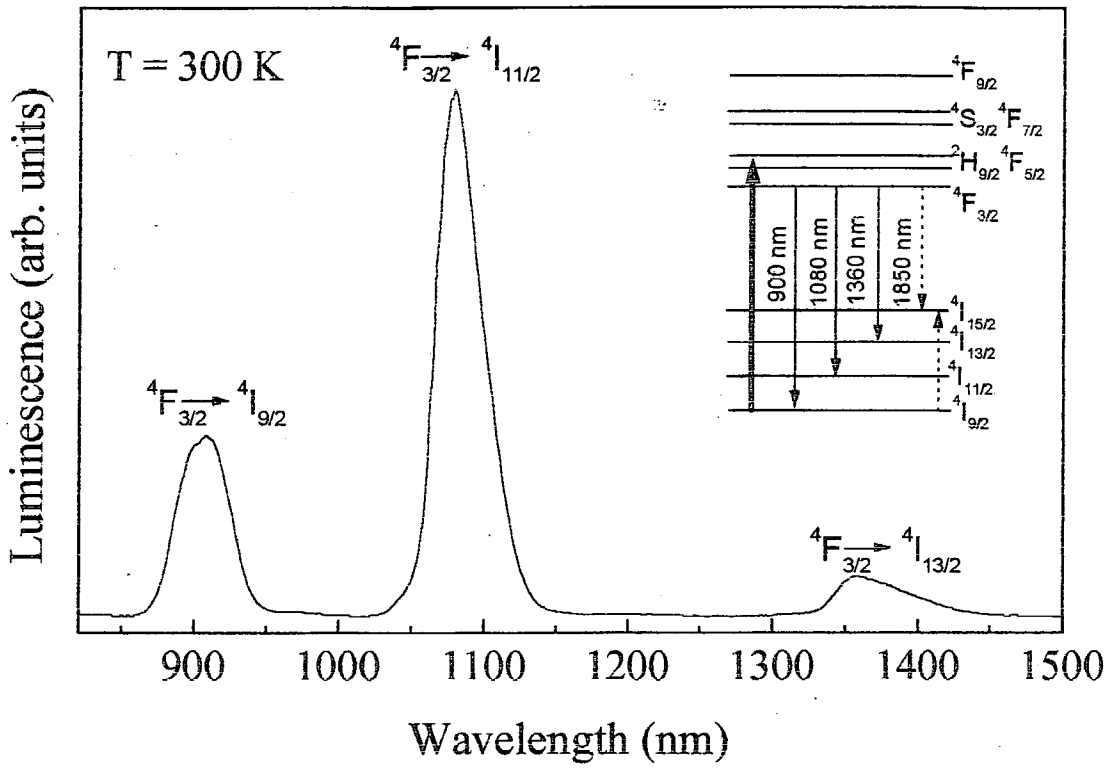

Figure 4: Lima et al.

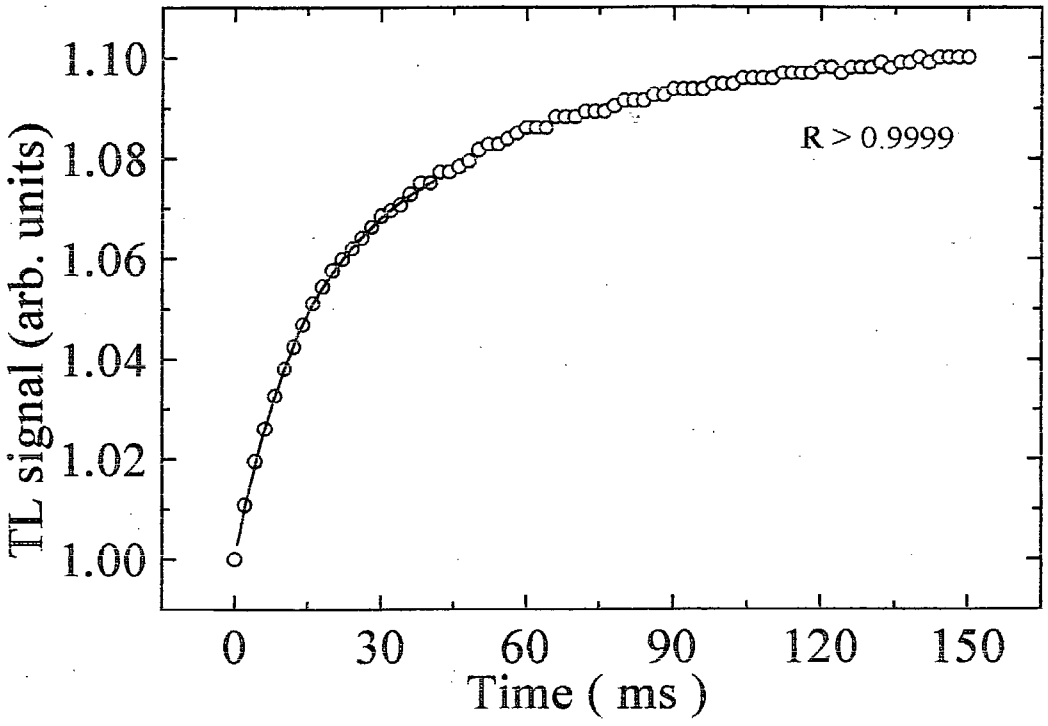

Figure 5: Lima et al.

Table Caption

Table 1: Experimental values of the physical parameters of chalcogenide glasses doped with Nd_2S_3. ρ is the density, H_v is the Vickers microhardness, α is the specific heat, T_g glass transition temperature and T_x glass crystallization temperature.

Table 2: Emission parameters and JO intensity parameters of Nd^{3+} doped GLS glass.

Table 3: Thermal diffusivity (D), thermal conductivity (K) and quantum efficiency (η) values obtained for Nd^{3+} doped GLS glass using thermal lens (TL) technique. The η values were also obtained using Judd Ofelt theory.

Sample %mol Nd_2S_3	ρ (± 0.004) gcm^{-3}	H_v $kgmm^{-2}$	α (± 0.04) $Jg^{-1}K^{-1}$	T_g (± 4) ^0C	T_x (± 4) ^0C
0.0	4.019	450 ± 18	0.54	544	657
0.05	4.047	458 ± 14	0.52	533	666
0.2	4.048	464 ± 27	0.54	538	669

Table 1: Lima et al.

Transition from $^4F_{3/2}$	λ (μm)	$A_{JJ'}$ (s^{-1})	$\beta_{JJ'}$ (%) (JO)	$\beta_{JJ'}$ (%) (exp.)
$^4I_{15/2}$	1.85	58.3	0.5	-
$^4I_{13/2}$	1.36	1179.0	7.5	8.5
$^4I_{11/2}$	1.08	6994.2	44	61.7
$^4I_{9/2}$	0.90	7477.2	48	29.8
	$\Omega_2 = (9.2 \pm 0.2) \times 10^{-20}$ cm^2			
	$\Omega_4 = (7.3 \pm 0.3) \times 10^{-20}$ cm^2			
	$\Omega_6 = (4.9 \pm 0.1) \times 10^{-20}$ cm^2			
	n = 2.4			
	$rms_{error} = 2\%$			

Table 2: Lima et al.

Sample %mol Nd_2S_3	D (± 0.1) cm^2s^{-1}	K (± 0.3) $WK^{-1}cm^{-1}$	η (± 0.08) (TL)	η (± 0.1) (JO)
0.0	2.7	5.9	-	-
0.05	2.7	5.9	1.01	1.00
0.2	2.7	5.9	1.03	0.96

Table 3: Lima et al.

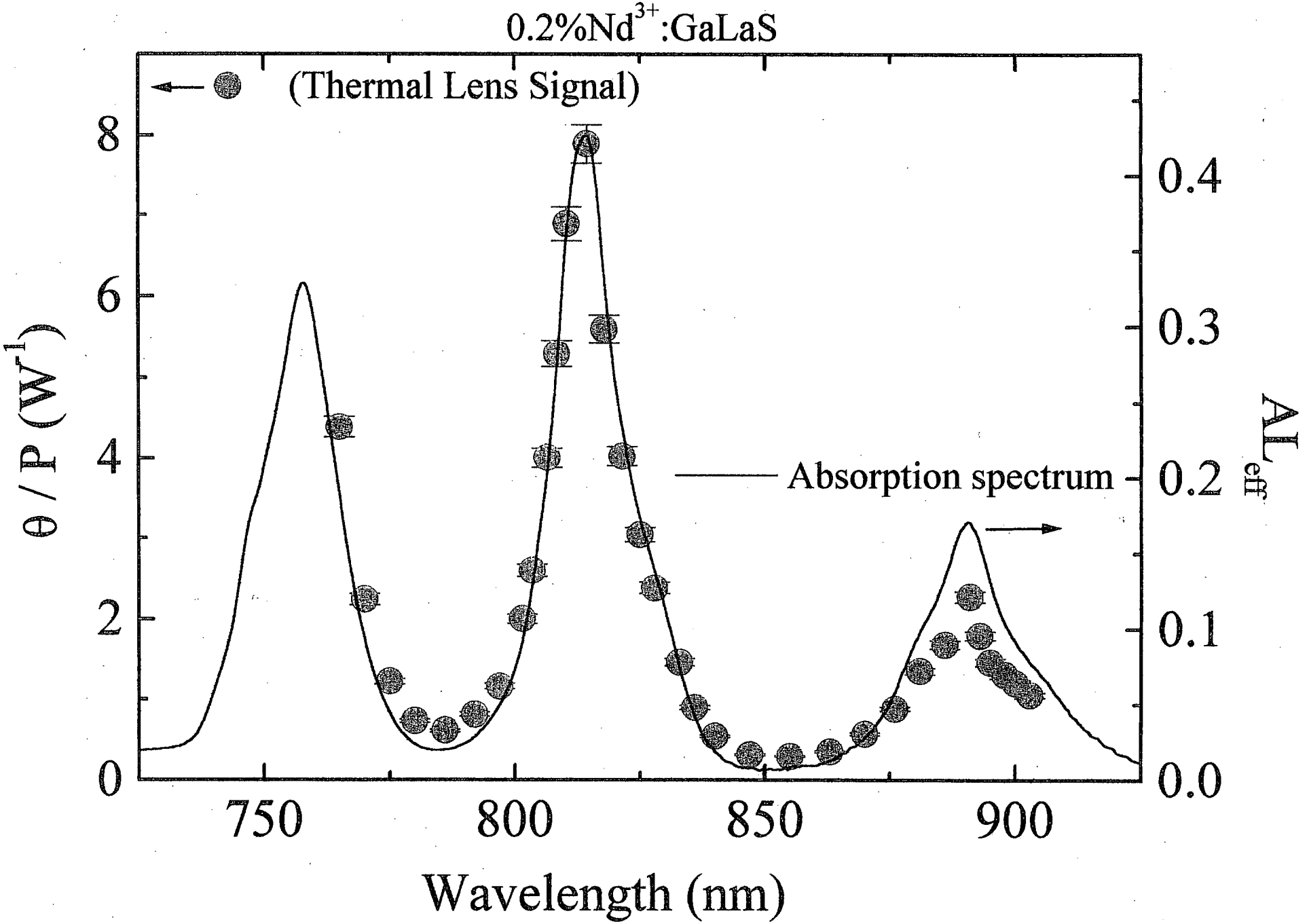
0.2%Nd3+:GaLaS
(Thermal Lens Signal)
Absorption spectrum
θ / P (W-1)
AL eff
Wavelength (nm)
0
2
4
6
8
0.0
0.1
0.2
0.3
0.4
750
800
850
900

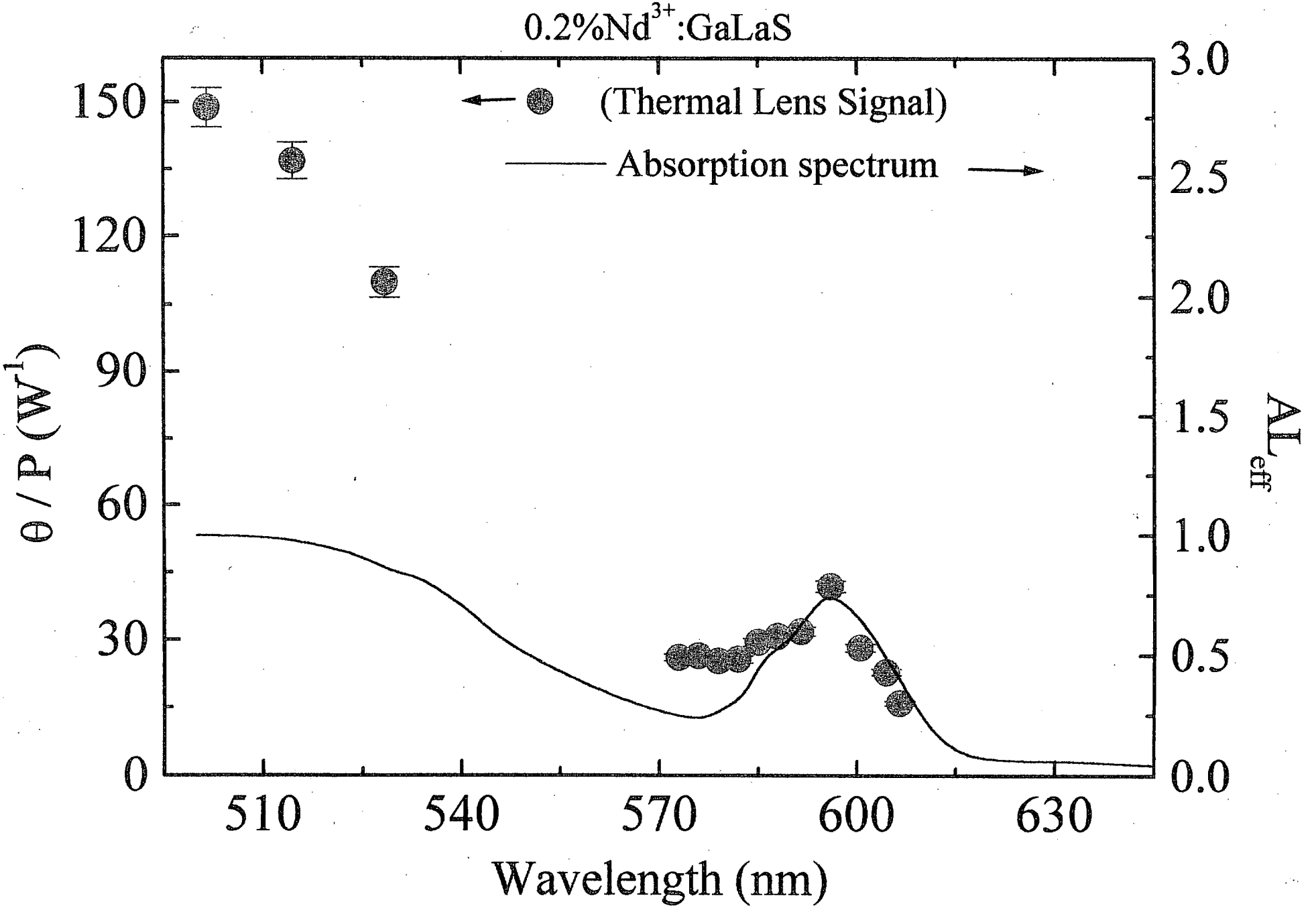
0.2%Nd3+:GaLaS
(Thermal Lens Signal)
Absorption spectrum
θ / P (W-1)
AL_eff
Wavelength (nm)
150
120
90
60
30
0
3.0
2.5
2.0
1.5
1.0
0.5
0.0
510
540
570
600
630

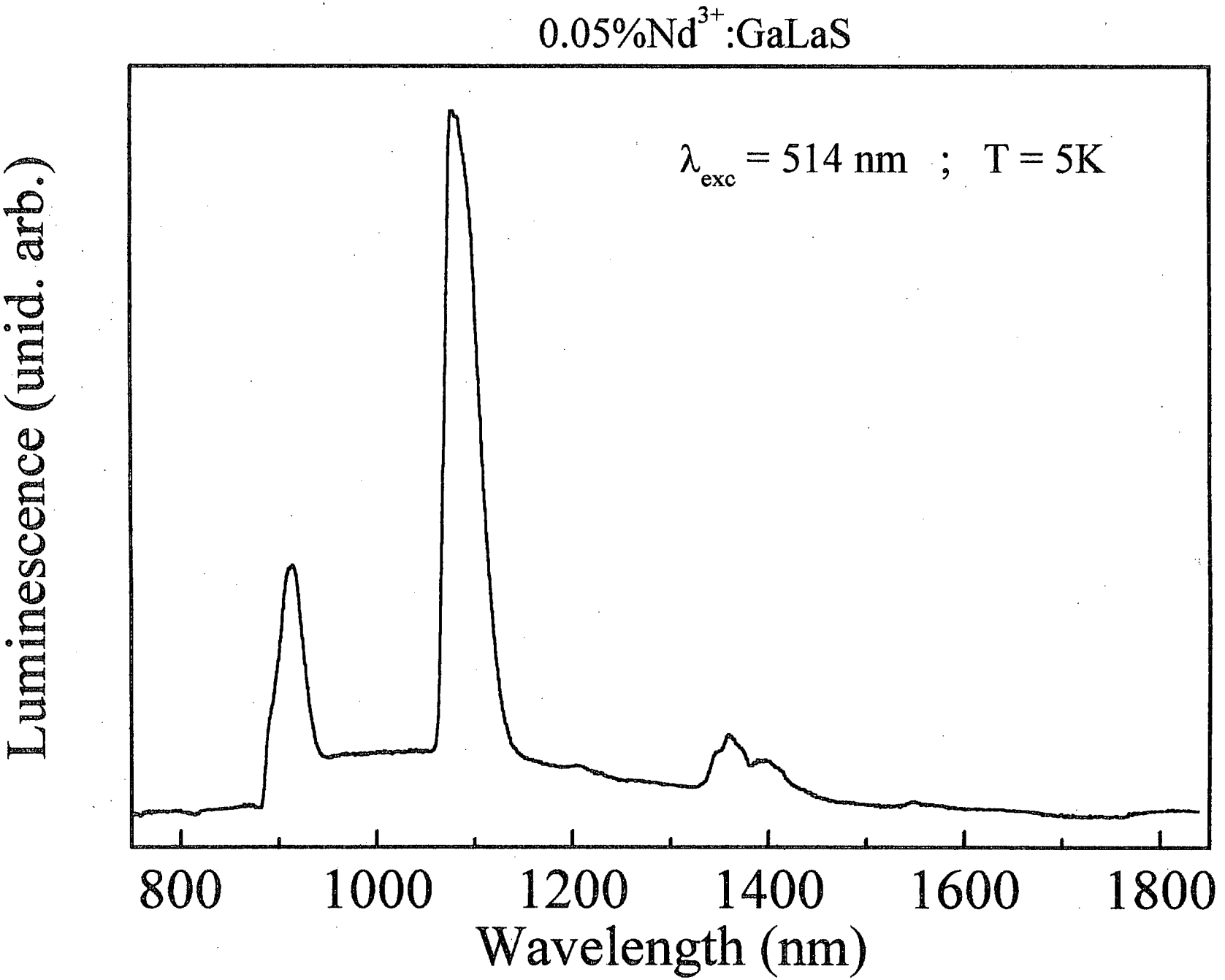
0.05%Nd3+:GaLaS
λexc = 514 nm ; T = 5K
Luminescence (unid. arb.)
800
1000
1200
1400
1600
1800
Wavelength (nm)

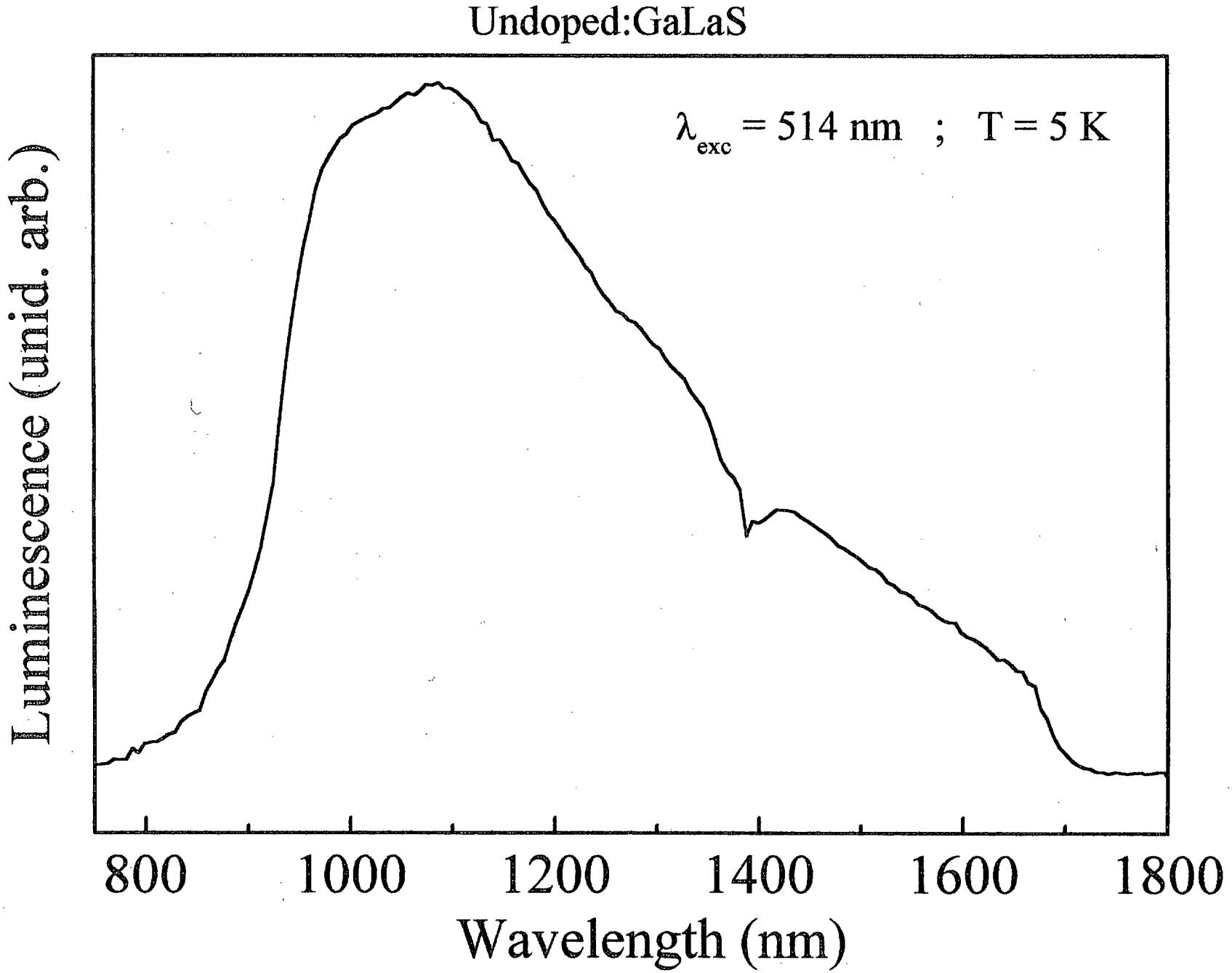
Undoped:GaLaS
λ_{exc} = 514 nm ; T = 5 K
Luminescence (unid. arb.)
800
1000
1200
1400
1600
1800
Wavelength (nm)

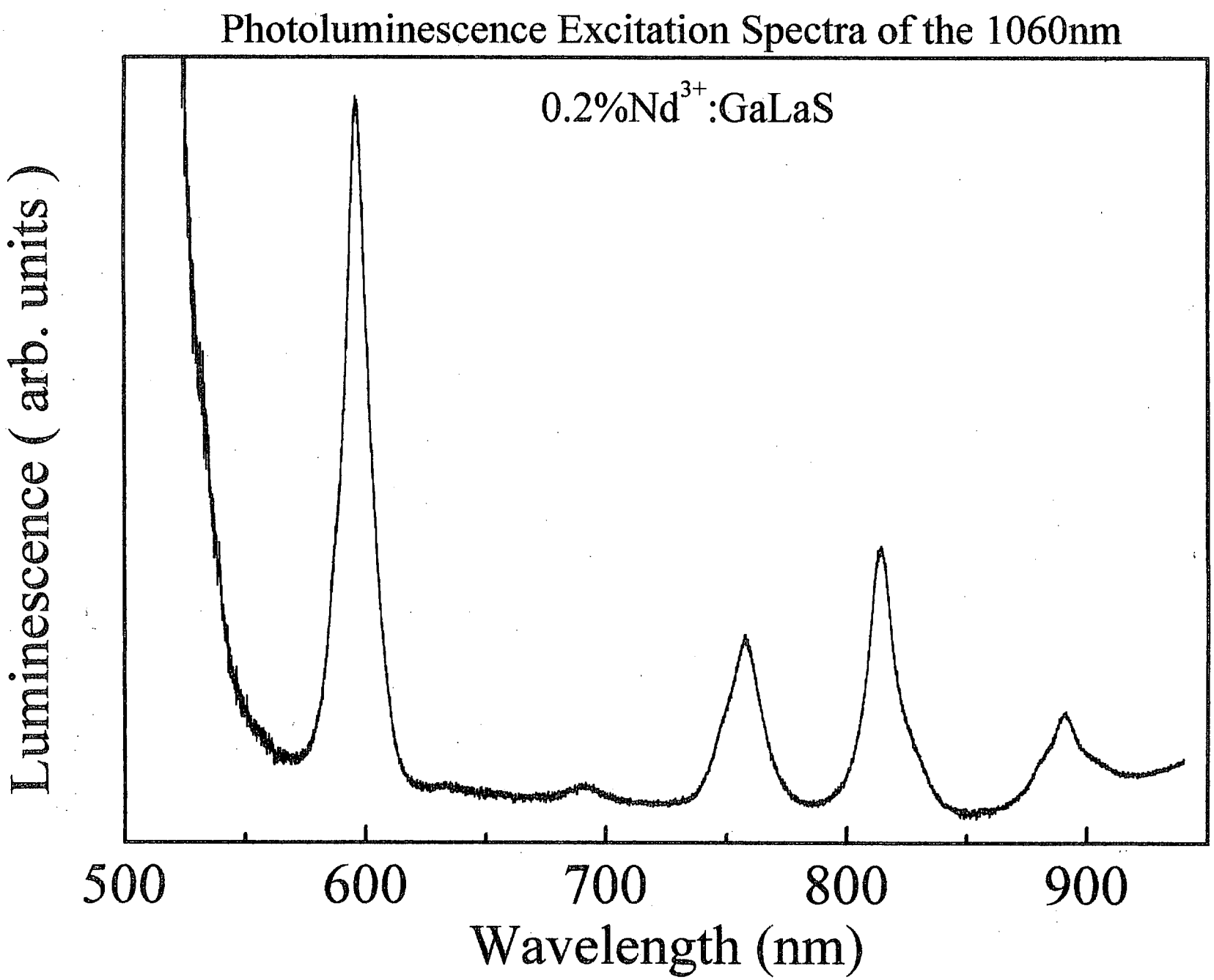
Photoluminescence Excitation Spectra of the 1060nm
0.2%Nd3+:GaLaS
Luminescence (arb. units)
500
600
700
800
900
Wavelength (nm)

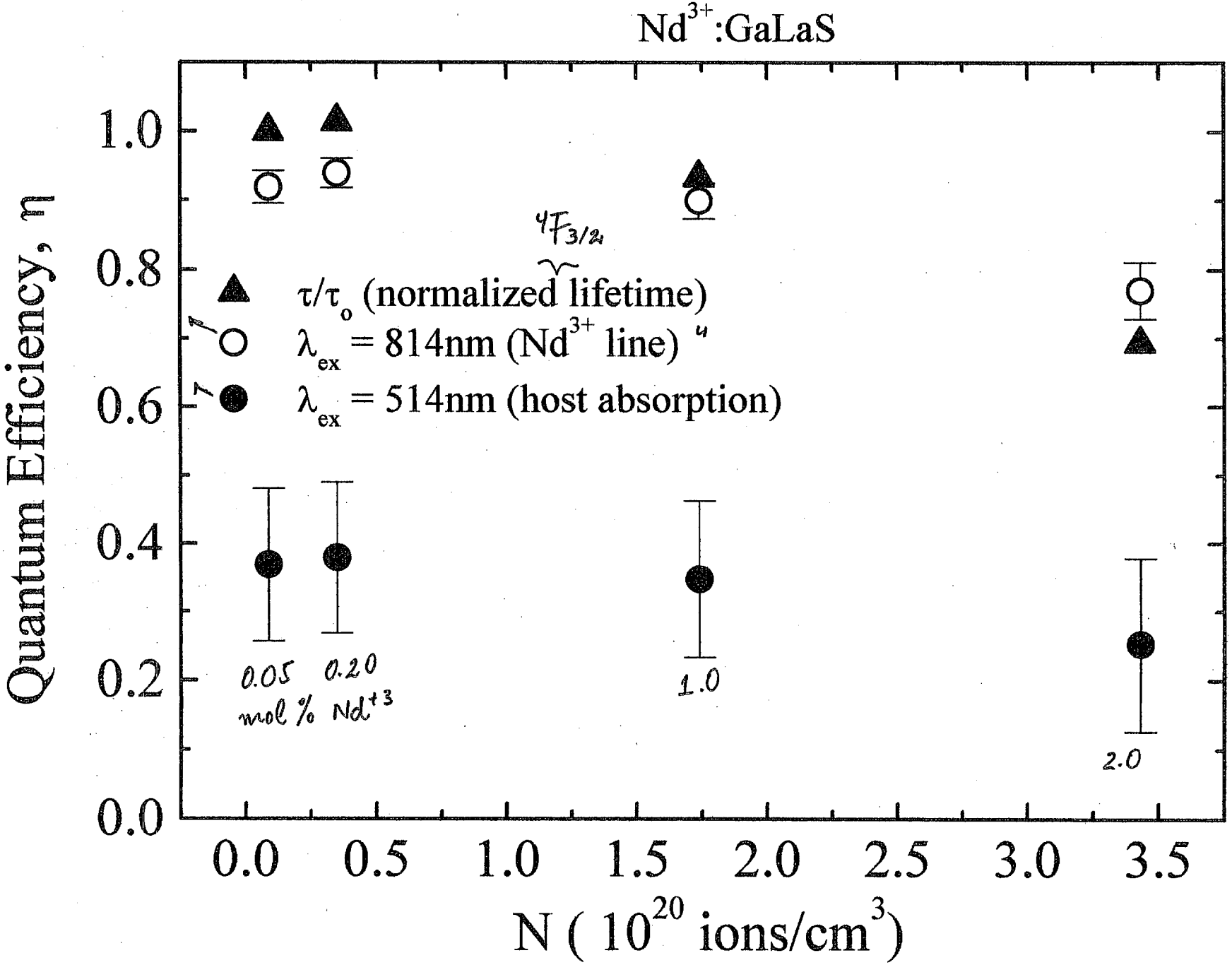
Nd3+:GaLaS
Quantum Efficiency, η
1.0
0.8
0.6
0.4
0.2
0.0
0.0
0.5
1.0
1.5
2.0
2.5
3.0
3.5
N (10^20 ions/cm^3)
4F3/2
τ/τo (normalized lifetime)
λex = 814nm (Nd3+ line)
λex = 514nm (host absorption)
0.05
0.20
mol % Nd+3
1.0
2.0